Journal of the European Ceramic Society 20 (2000) 765–773

The effect of compositional changes on the crystallization behaviour and mechanical properties of diopside–wollastonite glass-ceramics in the SiO_2–CaO–MgO (Na_2O) system

P. Alizadeh [a,*], V.K. Marghussian [b]

[a] *Ceramic Division, Material and Energy Research Centre, Tehran, Iran*
[b] *Ceramic Division, Department of Materials Science, Iran University of Science and Technology, Narmak, Tehran, Iran*

Received 15 February 1999; received in revised form 26 April 1999; accepted 13 May 1999

Abstract

The crystallization process of ternary system SiO_2–CaO–MgO (Na_2O) was investigated by DTA, XRD and SEM techniques and by strength measurements. The ability of $Cr_2O_3 + Fe_2O_3$ as nucleating agents in inducing bulk nucleation via formation of a spinel phase was proved. Wollastonite and diopside are two major phases that were identified after two-stage heat treatment. The spherulitic growth morphology was observed by SEM. At high growth temperatures for long times the recrystallization process was observed too. The kinetic parameters, such as activation energy and Avrami exponent, were calculated by Kissinger equation.

Keywords: Glass ceramics; Mechanical properties; Nucleating agents; Silicates

1. Introduction

Glass-ceramics are crystalline materials formed through the controlled crystallization of glass during specific heat treatment. The bulk chemical composition, nucleant added, final phase assemblage and microstructure are the most important factors affecting their technical properties. Crystallization of glass from the surface of a small number of sites in the interior usually results in low strength materials with coarse-grained microstructures. In contrast, efficient nucleation of crystals from numerous centres results in fine-grained microstructures and consequently high-strength materials. The role of nucleating agents in initiating glass crystallization from a multitude of centres was the major factor allowing the introduction of glass-ceramics into industrial applications.[1,2] The sintering production route for these materials is a major disadvantage and would make it relatively expensive and difficult to produce complex shapes. The classic glass-ceramic production route converting a monolithic glass to a monolithic ceramic is a more convenient method to fabricate these materials.

Furthermore, because the crystallization treatment commences in a homogenous glass, a glass-ceramic may be produced with an essentially zero porosity.[3]

Glass-ceramics obtained from crystallization of glass compositions located in ternary SiO_2–CaO–MgO system may contain several crystalline phases such as wollastonite, forsterite, diopside, protoenstatite and akermanite. Owing to the peculiar durability and mechanical properties of the phases present in these glass-ceramics, they may be suitable for many applications,[4] but initiation of internal bulk crystallization is relatively difficult in these glasses owing to nucleation problems.

In this work, the effect of compositional changes on crystallization behaviour of the ternary SiO_2–CaO–MgO(Na_2O) system, using a mixture of Cr_2O_3 and Fe_2O_3 as nucleating agents, was investigated. The growth morphologies were also studied and the activation energy of crystallization was calculated. The changes of mechanical properties versus composition of glasses was the other parameter that was investigated.

2. Experimental procedure

2.1. Glass preparation

The compositions of glasses studied are listed in Table 1. All of the raw materials used for preparation of the glasses were reagent grade. The weighed batch materials,

* Corresponding author.

0955-2219/00/$ - see front matter
PII: S0955-2219(99)00135-1

after thorough mixing were melted in a platinum crucible in an electric furnace at 1450°C for 1 h. The melts were then cast into hot stainless steel moulds. The glasses were annealed at 600°C for 2 h, and then furnace cooled to room temperature.

2.2. Heat treatment procedure

The thermal behaviour of glasses was monitored by DTA scans which were carried out using a simultaneous thermal analyser (Polymer Laboratories, STA-1640). For this purpose, 10 mg of the powder was sieved into fine and coarse fractions (63 and 180–212 μm, respectively) and analysed against Al_2O_3 powder as the reference material. In the experiment, a heating rate of 10°C min^{-1} in static atmosphere were maintained for all the DTA runs. Each glass sample was held at its appropriate nucleation and crystallization temperatures for 1–10 h. The heating rate was 5°C min^{-1} up to the nucleation temperature and 1°C min^{-1} between nucleation and crystallization temperatures.

2.3. Microstructural analysis

The microstructural studies, on the glass and the crystallized glass, were done by scanning electron microscope (Cambridge, Stereoscan 360). Crystalline phases present in glass-ceramic specimens were identified by X-ray powder diffractometer (Siemens, D-500).

Table 1
Compositions (wt%) of various glasses

Sample no.	SiO_2	CaO	MgO	Na_2O	Fe_2O_3	Cr_2O_3
1	59.68	21.23	6.02	5.08	4.00	4.00
2	59.68	18.23	9.02	5.08	4.00	4.00
3	59.68	15.23	12.02	5.08	4.00	4.00
4	59.68	12.23	15.02	5.08	4.00	4.00
5	59.68	9.23	18.02	5.08	4.00	4.00
6	59.68	6.23	21.02	5.08	4.00	4.00

Table 2
Crystallization peak temperatures for two particle sizes of various samples

Sample no.	% MgO	Particle size (μm)	T_p (°C)[a]	ΔT
1	6.02	< 63	910	
		180–212	935	25
2	9.02	< 63	891	
		180–212	931	40
3	12.02	< 63	886	
		180–212	931	45
4	15.02	< 63	894	
		180–212	918	24
5	18.02	< 63	880	
		180–212	907	27
6	21.02	< 63	872	
		180–212	906	34

[a] T_p, crystallization peak temperature.

2.4. Mechanical tests

Bending strength values were measured by four point loading method, using rectangular specimens (12×5×50 mm) and an Instron universal testing machine 1196. For each sample, six measurements were made in the air.

3. Results and discussion

3.1. Thermal analysis

The exothermic crystallization peak temperatures for glasses with different compositions and different particle sizes are tabulated in Table 2. In surface-nucleating glasses, the exothermic crystallization peak position is strongly dependent upon the particle size. The fine powders with high surface areas crystallized at lower temperatures. With efficient bulk nucleation the effect of particle size on the position of the exothermic peak should be low.[5]

In this way, for some compositions with relatively low difference in peak positions (e.g. 1, 4, 5), it seems that crystallization mainly could proceed by a bulk nucleation mechanism, and for specimen nos 2 and 3, for example, a surface crystallization mechanism may be operative. It also can be noted that increasing the content

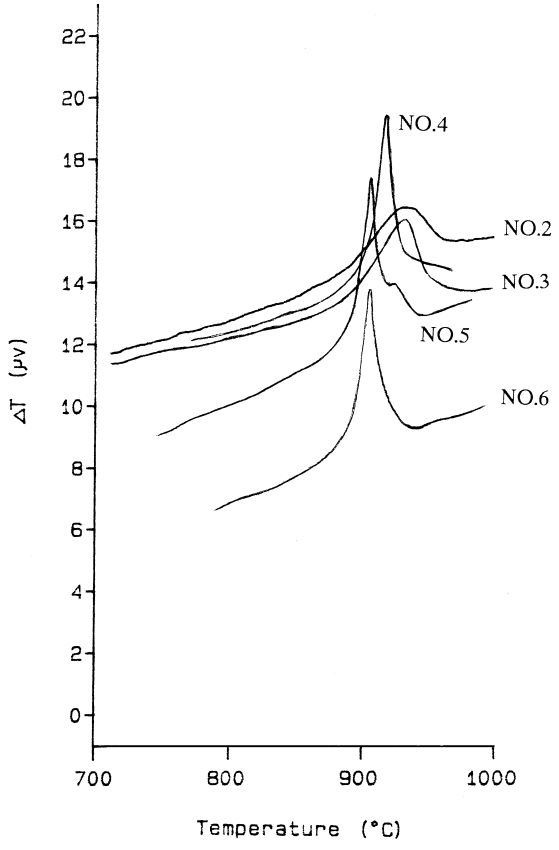

Fig. 1. DTA curves for sample nos 2–6.

of MgO at the expense of CaO resulted in the movement of the exothermic peak positions to lower temperatures in all glasses. This can be attributed to the gradual decrease of viscosity due to replacement of CaO by MgO. DTA curves for sample nos 2–6 are shown in Fig. 1.

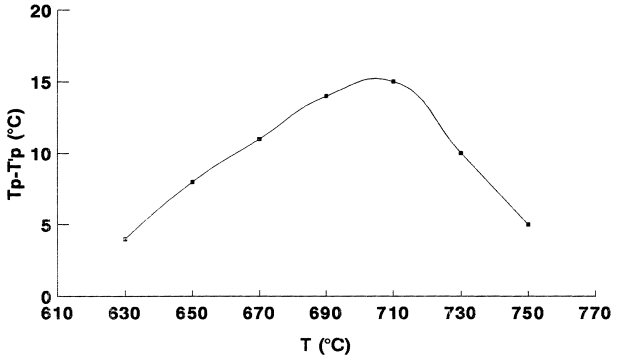

Fig. 2. T_p–T'_p plotted against temperature of heat treatment for sample no. 4 (T_p and T'_p are the crystallization peak temperatures of as-quenched and previously nucleated samples).

With attention to this figure, it is observed that the sample nos 2 and 3 (with $\Delta T = 40$ and 45°, respectively) have low intensity in DTA peaks, while DTA peaks due to sample nos. 4–6 are sharp. In this way, it seems that the latter samples with lower ΔT values have high susceptibility to crystallization.

For estimation of maximum nucleation rate temperature, the samples were first held for 2 h at different nucleation temperatures in 20°C intervals from T_g (glass transition temperature) to $T_g + 100$°C. The degree of shift of the crystallization peak to lower temperatures were then measured for these samples by DTA. The greatest shift of the crystallization peak indicates the optimum nucleation temperature.[6]

Fig. 2 shows the variation of the shift ($T_p - T'_p$) versus nucleation temperature for sample no. 4, where T_p and T'_p are the crystallization peak temperatures of as-quenched and previously nucleated samples, respectively. In this way, the maximum nucleation temperature was found as 710°C. The limitation of growth temperatures for bulk samples were found as 920 to 960°C.

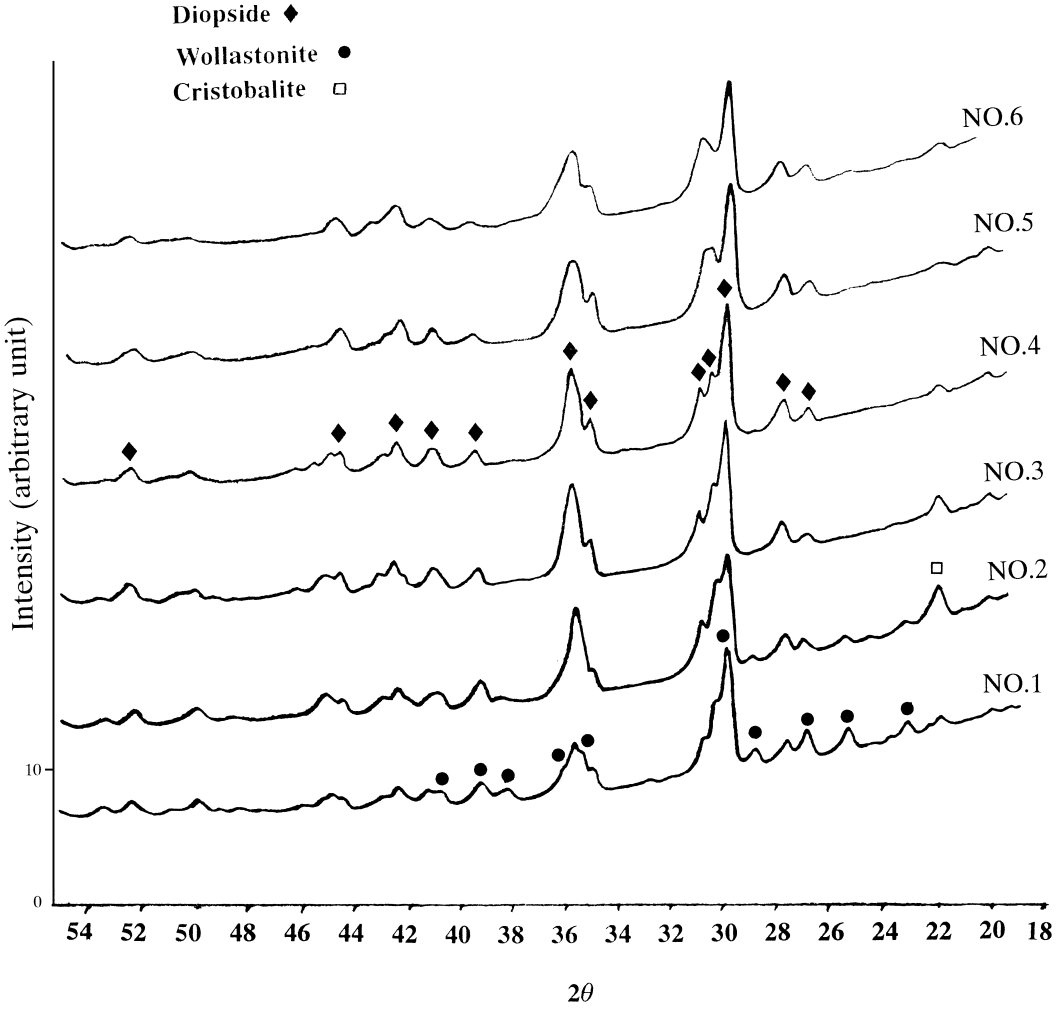

Fig. 3. XRD patterns of glass-ceramics after heat treatment at 710 and 960°C for 3 h.

3.2. XRD analysis

Fig. 3 shows the XRD patterns for all specimens after heat treatment at mentioned temperatures for 3 h. The results of X-ray analysis of glass-ceramics are also tabulated in Table 3. It is seen that as expected, increasing the content of MgO at the expense of CaO resulted in a decrease of the peak intensity of wollastonite and an increase in diopside phase. A small peak with low intensity due to cristobalite phase can also be observed. Furthermore, it is observed that the width of peaks were broader in sample nos 5 and 6. Referring to the wide range of ionic substitutions present in the monoclinic pyroxene,[7] the broadening of peaks could be attributed to replacement of Ca^{+2} and Mg^{2+} by Na^{+}, Fe^{+2}, Fe^{+3} and Cr^{+3} ions. On the other hand, it seems that with increase of MgO content, the formation of other silicate phases is also responsible for the broadening of peaks.[8]

Table 3
Crystalline phases in various samples

Sample no.	Crystalline phases
1	Wollastonite–diopside–cristobalite[a]
2	Wollastonite[a]–diopside–cristobalite
3	Diopside–cristobalite
4	Diopside–cristobalite
5	Diopside–cristobalite[a]
6	Diopside–cristobalite[a]

[a] Minority phases.

3.3. Microscopic examinations

Fig. 4 shows the micrographs of specimen no. 1 after crystallization, taken by SEM at two different magnifications. These figures revealed wollastonite particles (light colour) along with fibrous crystals of diopside (dark colour).

Fig. 5 shows the micrographs of specimen no. 2 after crystallization, at two different magnifications. This figure revealed the spherulitic growth morphology for internally nucleated diopside. The extensive phase separation after 2 h at the nucleation temperature in the case of glass sample no. 2 is shown in Fig. 6.

According to McMillan,[9] chromium in the hexavalent state (Cr^{+6}) has a higher field strength and hence it

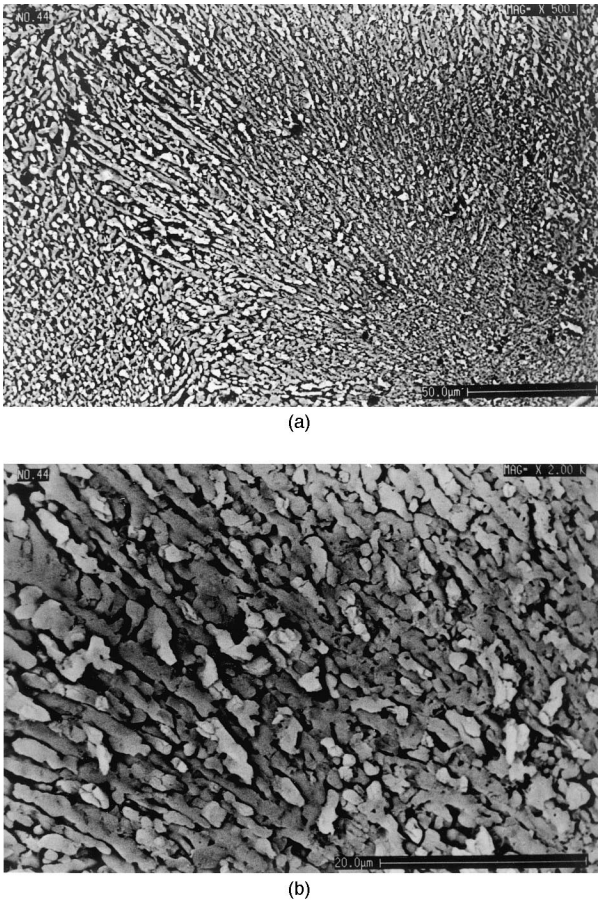

Fig. 4. SEM micrographs of crystallized sample no. 1: (a) magnification×500; (b) magnification×2000.

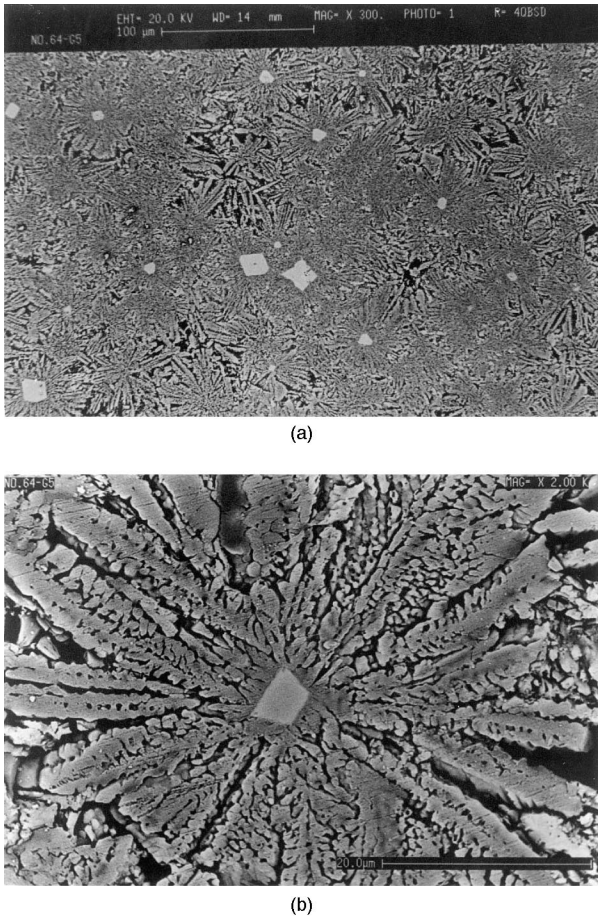

Fig. 5. SEM micrographs of crystallized sample no. 2: (a) magnification×300; (b) magnification×2000.

would occupy an interstitial position, exerting a marked ordering effect upon the oxygen ions surrounding it. Thus, the amorphous chromium-rich phase separates out from the glass. The EDAX analysis of sample no. 2 at the central region of the spherulite, which is distinguishable with its light colour (Fig. 5), showed the spinel phase, $(Mg, Fe)(Fe, Cr)_2O_3$ (Fig. 7). This phase, which can readily be crystallized out from the chromium-rich glassy phase, may act as crystallization centres or nuclei for the main crystalline phases.[10] In this way it seems that sample no. 2 with $\Delta T = 40$ has the simultaneous capability of surface and bulk nucleation.

The other nucleating agent, Fe_2O_3, has probably improved both the nucleation and growth rates of crystalline phases not only by contributing to spinel phase formation and favourably altering its lattice constant,[11] but also by decreasing viscosity of the initial glass.

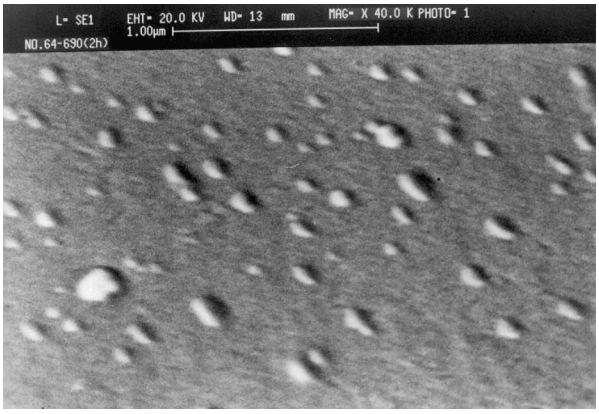

Fig. 6. Phase separation after 2 h at 710°C for glass sample no. 2.

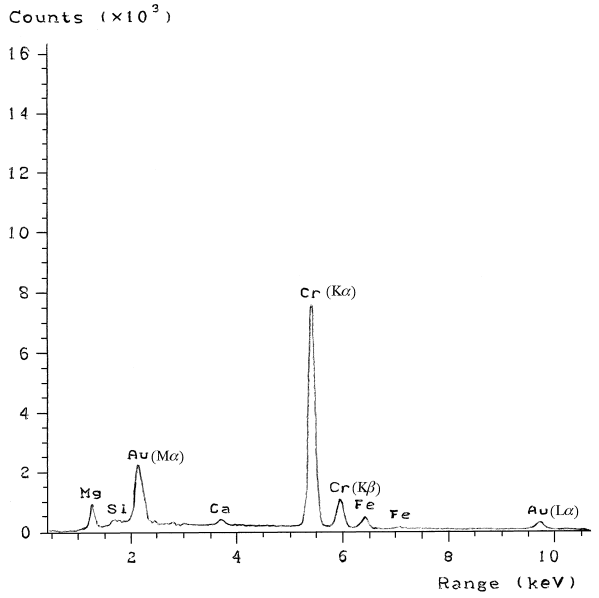

Fig. 7. EDAX analysis of spinel phase at the central region of the spherulites.

3.3.1. Growth morphology

In addition to sample no. 2, the spherulitic growth morphology can also be seen for sample nos 3 and 4 in Figs. 8 and 9, respectively. For many materials having high entropies of fusion, undergoing crystallization at large undercoolings, nucleation of new crystals having different orientation can occur either at or in advance of

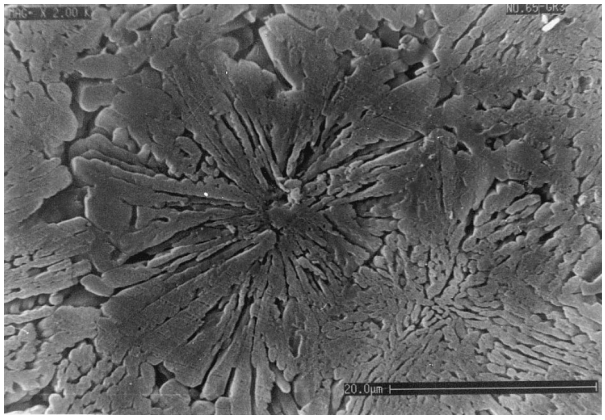

Fig. 8. SEM micrograph of crystallized sample no. 3.

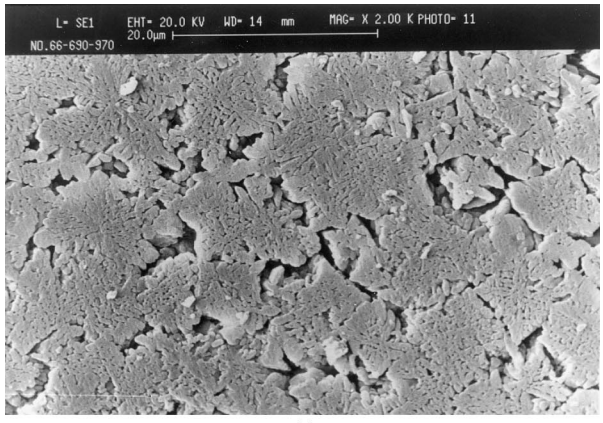

(a)

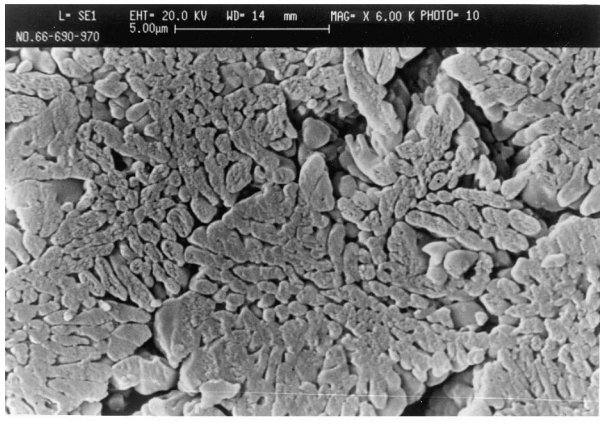

(b)

Fig. 9. SEM micrographs of crystallized sample no. 4: (a) magnification×2000; (b) magnification×6000.

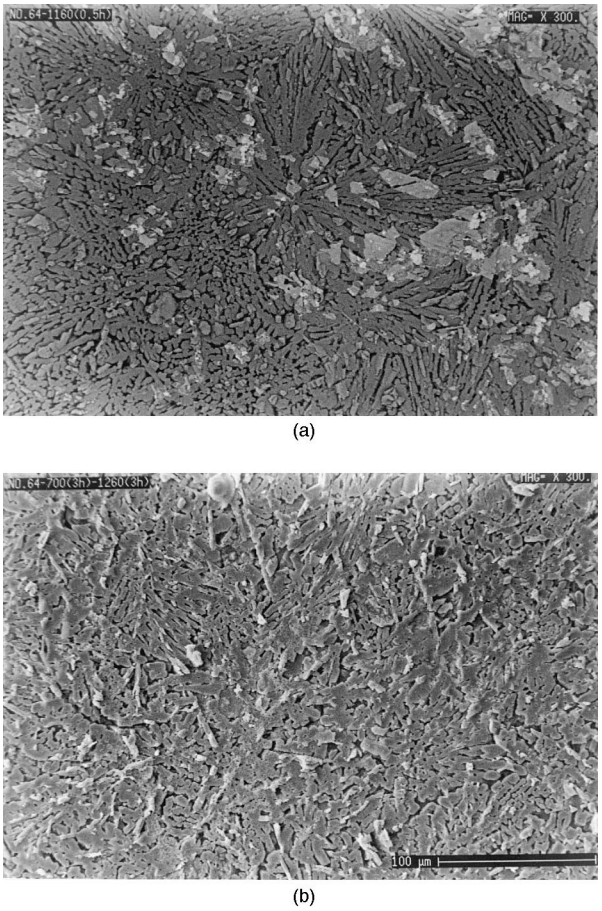

Fig. 10. Recrystallization in glass-ceramic no. 2: (a) heat treated at 1160°C for 0.5 h; (b) heat treated at 1260°C for 3 h.

the growth front. This type of nucleation can result in spherulitic growth. All spherulites comprise fibrous crystals radiating from a common centre.[9]

The crystallographic orientation and the growth direction of the branches, which always develop at low angles to the original fibre, are controlled by the interference of the diffusion fields of adjacent branches.[12]

3.3.2. Recrystallization

All microstructures, which contain fibrillar morphologies, can be recrystallized when annealed at high temperatures for long times. In order to observe this phenomenon the glass sample no. 2 was heat treated at 1160 and 1260°C for 1/2 and 3 h, respectively. It is seen that the recrystallization has been started in the sample heat treated at 1160°C for 1/2 h [Fig. 10(a)], but some spherulites still persisted. After 3 h soaking at 1260°C, it seems that the recrystallization has been completed [Fig. 10(b)]. After recrystallization in both samples large voids appeared which were observable even by normal visual inspection. The XRD pattern of this sample after 3 h heat treatment at 1260°C showed that major crystalline phase existing in the sample was diopside (Fig. 11).

Density measurements showed that the density of latter glass-ceramic was higher than the parent glass in this sample (for example, the densities of glassy sample no. 2 and its glass-ceramic counterpart were found to be 2.68 and 3.31 Mg m^{-3}, respectively).

The densities of diopside and wollastonite are 3.39 and 2.8, respectively. Therefore it is expected that the samples containing diopside as the major crystalline

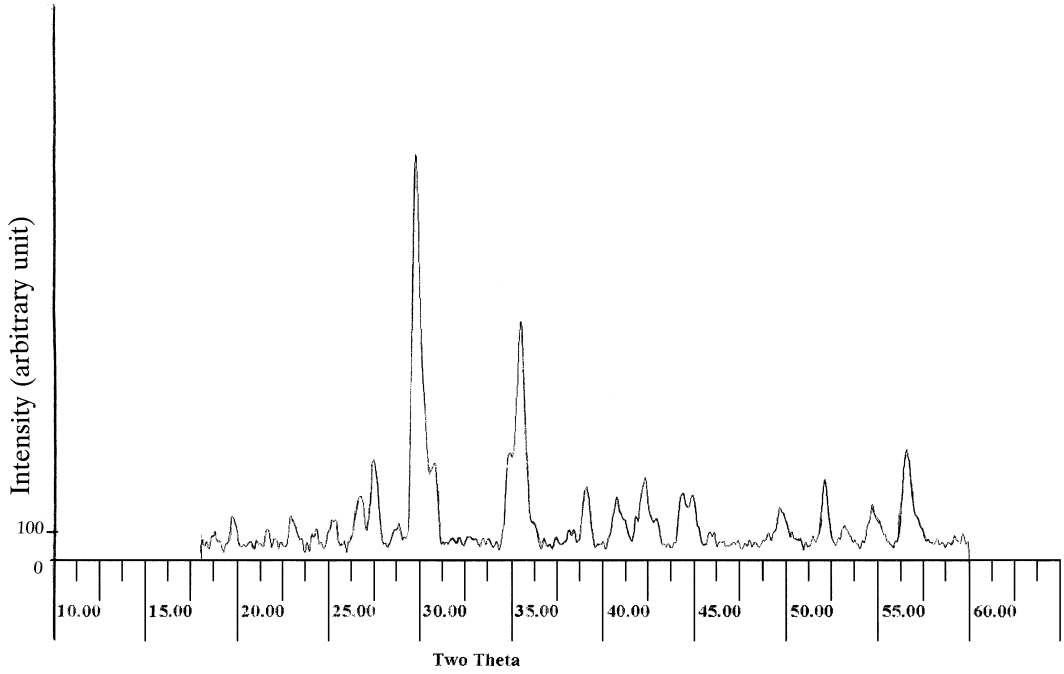

Fig. 11. XRD pattern of glass-ceramic after 3 h heat treatment at 1260°C.

phase are generally more susceptible to pore formation owing to the density differences between crystalline phase and glassy residue.

It seems that the main driving force for recrystallization process stems from a reduction in the large surface area of the fibrils.[13,14]

3.4. Mechanical tests

The variations of bending strength versus time of nucleation and growth for specimen no. 2 are shown in Fig. 12. It is observed that increasing the time of nucleation and growth results in increasing the bending strength at first and decreasing thereafter. The improvement of bending strength with nucleation time up to 5 h is mainly attributed to the increase in the volume of wollastonite and diopside. With higher times of nucleation, on the other hand, decrease of bending strength can be attributed to the probable coalescence of existing nuclei, giving rise to smaller nuclei population. Decrease of bending strength at higher growth times could be due to increasing the spherulite size.

The value of bending strength versus MgO percentage is given in Fig. 13. It can be seen that the bending strength was decreased with increasing MgO content. It seems that the difference in density between diopside and residual glass is responsible for this observation.

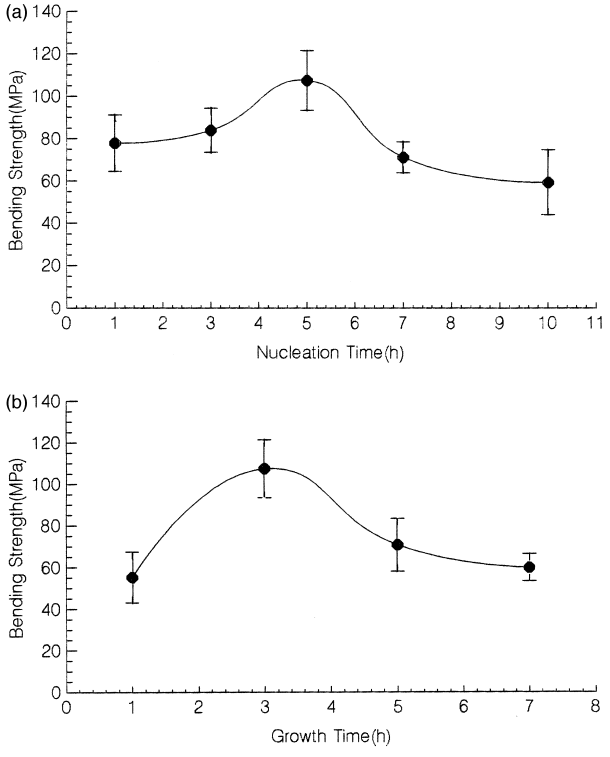

Fig. 12. (a) Variations of bending strength versus times of nucleation at 710°C for sample no. 2, with 3 h growth at 960°C; (b) variations of bending strength versus times of growth at 960°C for sample no. 2, with 5 h nucleation at 710°C.

Since some samples exhibited large bubbles even before crystallization, it was postulated that this can be related to more severe phase separation occurring in high percentages of MgO. This phenomenon resulted in higher viscosities,[15] which prevents the escape of gases during glass melting and casting.

In our opinion this phenomenon along with density difference is responsible for pore formation and lower strengths in the specimens with higher MgO contents.

3.5. Activation energy determination

The DTA curves can be used to determine the activation energy for crystal growth by analysing the exothermic peaks on the basis of the nucleation and growth equation.[16]

DTA runs were performed at different heating rates ($\alpha = 10$–50 K min^{-1}) and the peak position shifts were measured.

The activation energy for crystal growth, E_c and the Avrami exponent, n, were then determined according to the modified Kissinger and the modified JMA equations,[17,18] [Eqs. (1) and (2), respectively]:

$$\mathrm{Ln}\left(\frac{\alpha^n}{T_p^2}\right) = -\frac{mE}{RT_p} + \text{constant} \quad (1)$$

where T_p and α are crystallization peak temperature and heating rate, respectively.

$$\mathrm{Ln}[-\mathrm{Ln}(1-x)] = -n\mathrm{Ln}\alpha - m\frac{E_c}{RT} + \text{constant} \quad (2)$$

where x is the fraction crystallization, m and n are integers, the values of which depend on the growth mechanism. The value of n can be calculated at any fixed temperature from the plot of $\mathrm{Ln}[-\mathrm{Ln}(1-x)]$ versus Ln α. This value was calculated for specimen no. 4 as 2.3 [Fig. 14(a)]. This value indicates a crystal growth mechanism in two to three dimensions (with fibre shape

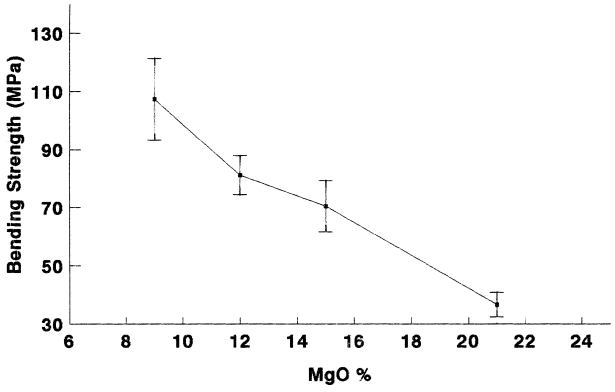

Fig. 13. Variations of bending strength versus MgO percentage in sample nos 2–6 after heat treatment at 710° for 5 h and at 960°C for 3 h.

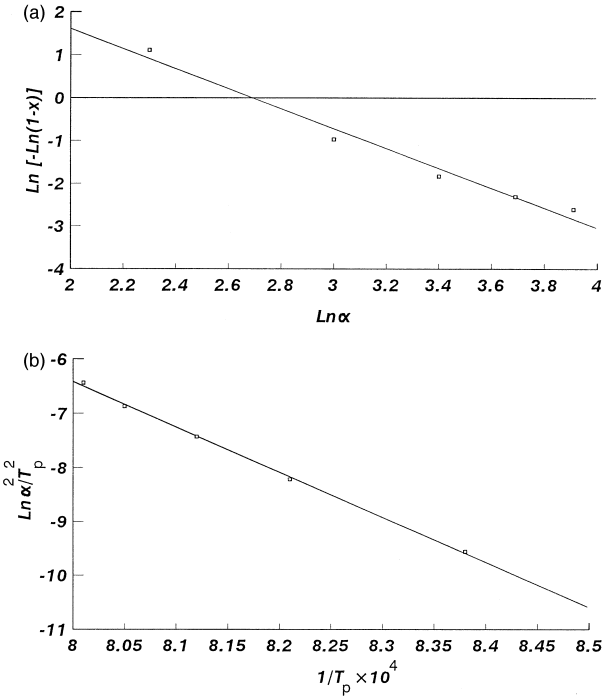

Fig. 14. (a) Plot of Ln $[-\mathrm{Ln}(1-x)]$ versus Lnα for sample no. 4; (b) plot of the so-called modified Kissinger equation for sample no. 4.

particle that grow radially). When nucleation occurs during the DTA runs, $m = n - 1$, thus $m = 1$ for this case.

According to eqn (1), the E_c value can be obtained from the slope of the plot $\mathrm{Ln}\dfrac{\alpha^n}{T_p^2}$ versus $1/T_p$. This value was about 693.2 kJ mol^{-1} for specimen no. 4 [Fig. 14(b)].

For sample no. 2, the values of n and E_c were obtained as 1 and 395.9 kJ mol^{-1}, respectively. $n = 1$ indicates surface crystallization mechanism in sample no. 2. On the other hand, by a comparison between the values of E_c for sample nos 2 and 4, it is concluded that activation energy for surface crystallization is generally lower than that for bulk crystallization.[19]

4. Conclusions

1. The ability of 4 wt% Cr_2O_3 + 4 wt% Fe_2O_3 nucleating agents in inducing bulk nucleation via formation of a spinel phase was proved for all compositions investigated herein.
2. All specimens showed a certain degree of bulk nucleation, despite the relatively large ΔT values revealed by some specimens. No distinct surface crystallization was observed, contrary to earlier expectations. However, the sharpness of DTA peaks for some specimens coinciding with lower ΔT values indicates their higher susceptibility to bulk nucleation, whereas in the case of specimens exhibiting broader DTA peaks simultaneous surface and bulk nucleation may be operative.
3. The spherulitic growth morphology for diopside was observed in most specimens investigated herein.
4. The recrystallization process was observed after heat treatment at high growth temperatures for long times. In this process, the spherulitic morphology disappeared and a fine microstructure was formed. The increase of crystalline phases (especially diopside) due to this high temperature heat treatment caused pore growth and decrease of strength nullifying the effect of fine microstructure.
5. The increase of MgO content generally resulted in lower strength values. This was related to pore growth process owing to difference in density between crystals and residual glass and also to the phase separation in the glass phase increasing viscosity.
6. The kinetic parameters, such as activation energy and Avrami exponent were calculated as 693.2 kJ mol^{-1} and 2.3, respectively, for a sample containing 15% MgO. The later value indicates a crystal growth mechanism in three dimensions. For sample containing 9% MgO, these values were calculated as 395.9 kJ mol^{-1} and 1, respectively. For this sample, surface crystallization is the dominant mechanism.

References

1. Beall, G. H., Design of glass-ceramics. *Reviews of Solid State Science*, 1989, **3**, 333–354.
2. Omar, A. A., El-Shennawi, A. W. A. and Khater, G. A., The role of Cr_2O_3, LiF and their mixtures on crystalline phase formation and microstructure in Ba, Ca, Mg alumino silicate glass. *Br. Ceram. Trans. J.*, 1991, **90**, 179–183.
3. Carpenter, P. R., Campbell, M., Rawlings, R. D. and Rogers, P. S., Spherulitic growth of apatite in a glass-ceramic system. *J. Mat. Sci. Lett.*, 1986, **5**, 1309–1312.
4. Baldi, G., Generali, E. and Leonelli, C., Effects of nucleating agents on diopside crystallization in new glass-ceramics for tile-glaze application. *J. Mat. Sci.*, 1995, **30**, 3251–3255.
5. Hill, R. and Wood, D., Apatite–mullite glass-ceramics. *J. Mat. Sci., Mat. Med.*, 1995, **6**, 311–318.
6. Bryden, R. H. and Caley, W. F., Determination of nucleation temperature of a lime alumino silicate glass-ceramic by differential thermal analysis. *J. Mat. Sci. Lett.*, 1997, **16**, 56–58.
7. Putnis, A., *Introduction to Mineral Sciences*. Cambridge University Press, 1992.
8. Alizadeh, P. and Marghussian, V. K., Effect of nucleating agents on the crystallization behaviour and microstructure of SiO_2–CaO–MgO(Na_2O) glass-ceramics. *J. Eur. Ceram. Soc.*, in press.
9. McMillan, P. W., *Glass-ceramics*. Academic Press, 1979.
10. Barbieri, L., Leonelli, C. and Manfredini, T., Solubility, reactivity and nucleation effect of Cr_2O_3 in the CaO–MgO–Al_2O_3–SiO_2 glassy system. *J. Mat. Sci.*, 1994, **29**, 6273–6280.

11. Ying, Y. X. and Cable, M., Mossbauer study of crystallization of glasses in the system K_2O–Na_2O–CaO–MgO–Al_2O_3–SiO_2. *J. Mat. Sci*., 1992, **27**, 1137–1141.
12. Barry, T. L., The mineralogy of glass-ceramics. *Proc. Brit. Ceram. Soc*., 1979, **28**, 1–22.
13. Lewise, M. H., Metcalf-Johansen, J. and Bell, P. S., Crystallization mechanisms in glass-ceramics. *J. Am. Ceram. Soc*., 1979, **62**, 278–288.
14. Lewis, M. H. and Smith, G., Spherulitic growth and recrystallization in barium silicate glasses. *J. Mat. Sci*., 1976, **11**, 2015–2026.
15. Mazurin, O. V. and Porai-Koshits, E. A., *Phase Separation in Glass*. North-Holland Physics Publishing, The Netherlands, 1984.
16. Bansal, N. P. and Doremus, R. H., Determination of reaction kinetic parameters from variable temperature DSC or DTA. *J. Am. Ceram. Soc*., 1983, **66**, 233–237.
17. Sung, Y. M., The effect of additives on the crystallization and sintering of $2MgO$–$2Al_2O_3$–$5SiO_2$ glass-ceramics. *J. Mat. Sci*., 1996, **31**, 5421–5427.
18. Matusita, K. and Sakka, S., Kinetic study on crystallization of glass by differential thermal analysis — criterion on application of Kissinger plot. *J. Non-Cryst. Solids*, 1980, **38–39**, 741–746.
19. Ovecoglu, M. L., Kuban, B. and Ozer, H., Characterization and crystallization kinetics of a diopside-based glass-ceramic developed from glass industry raw materials. *J. Eur. Ceram. Soc*., 1997, **17**, 957–962.